Critical currents in sputtered Nb-Ta multilayers

P. R. Broussard

Naval Research Laboratory, Washington, D.C. 20375-5000

T. H. Geballe*

Department of Applied Physics, Stanford University, Stanford, California 94305

(Received 18 May 1987; revised manuscript received 7 August 1987)

Critical-current measurements have been made on sputtered Nb-Ta multilayers for both perpendicular and parallel applied field. For large bilayer periods, the pinning force behaves as $h(1-h)$ and is due to dislocation pinning. As the bilayer period decreases, the pinning force decreases and changes over to a collective mechanism. For parallel applied field, there is a lack of temperature scaling and an increase in the pinning force, which is due to pinning by the multilayering. A search for the existence of other effects is discussed.

INTRODUCTION

Critical-current measurements on multilayered systems have formed a sparse field of work, with data published mainly on metal-insulator systems[1] and on the Pb-Bi system.[2] Theoretical studies[3] have predicted many varied effects in multilayered systems, such as enhanced current densities, synchronous pinning, etc. We have measured critical currents and pinning forces for sputtered Nb-Ta multilayered films in the hope of observing the effects of the layering on the critical current and flux-pinning force. Measurements of the transition temperature and upper critical field for these samples have been previously reported.[4,5]

SAMPLE PREPARATION

The sample preparation is given in Ref. 4. The multilayers were prepared by magnetron sputtering from separate Nb and Ta sources onto different orientations of epitaxially polished sapphire substrates at elevated substrate temperatures. The background pressure was 3×10^{-7} Torr with N_2 and H_2 being the predominant residual gases. The argon pressure used during sputtering was 2 mTorr, and the deposition rates were typically 10–15 Å/s.

The samples in this study are broken down into two sets. The first set (I) have a nearly constant tantalum layer thickness (≈ 500 Å), and the niobium layer thickness is varied from 98 to 490 Å. These samples (which were studied in Ref. 4, and labeled 7, 8, and 9 there) were primarily used to study how critical currents varied as the applied field changed from being perpendicular to the layers to being parallel. The second set (II), studied in Ref. 5, has a constant niobium to tantalum layer thickness ratio (1.3), but the bilayer period $(\Lambda = d_{Nb} + d_{Ta})$ is varied from 19.5 to 228 Å. These samples were used to examine the effect of the bilayer period on the critical current. Routine sample characterization (x rays and resistivity) as well as critical-field results are

discussed in Refs. 4 and 5, and only directly relevant information will be discussed here.

CRITICAL-CURRENT MEASUREMENTS

For critical-current-density (J_c) measurements, the samples (≈ 5000 Å thick) were patterned into a four-point bridge, 70 μm wide. J_c was measured with the field either perpendicular or parallel to the layers, and with the magnetic field perpendicular to the current at all times. A transport method was used to measure J_c: at a constant temperature and magnetic field, the applied current is increased slowly until a 1-μV potential difference appears across the voltage contacts which are separated by 1800 μm. This definition was chosen since the I-V curves for these samples do not exhibit classical flux flow behavior. There has been much discussion on the definition of J_c by transport measurements,[6] but in our system, the actual choice for the voltage criterion makes a difference only very near $J_c = 0$. From the obtained value of I_c, we define J_c by using the entire film cross section. This definition is merely one of convenience, as the actual distribution of current in the multilayer is not known. Due to sample heating problems, currents had to be limited to less than 100 mA. From the applied magnetic field and this current density, we define the flux-pinning force in the usual method,

$$F_p = \frac{1}{c} |\mathbf{J}_c \times \mathbf{B}| \ .$$

For the samples in set I, $J_c(H)$, and $F_p(H)$ were measured for parallel and perpendicular fields at three different temperatures. For set II samples, the measurements of $J_c(H)$ and $F_p(H)$ were looked at primarily for the case of perpendicular field.

H PERPENDICULAR TO THE LAYERS

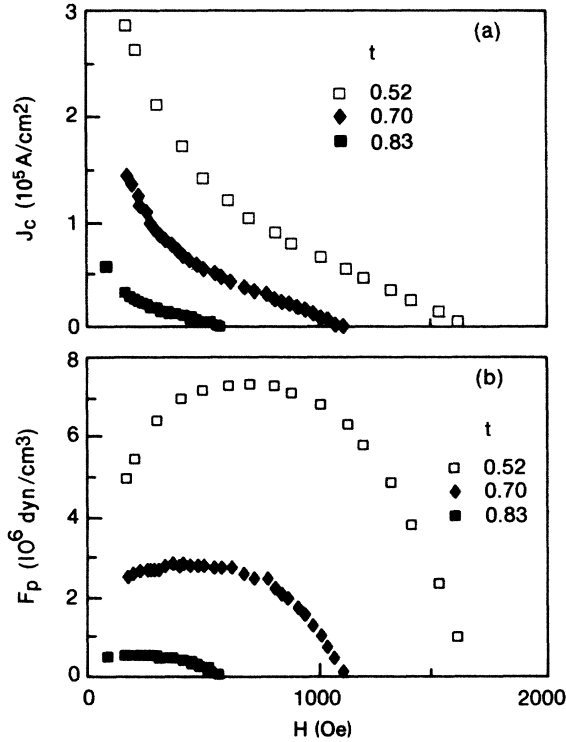We first look at the results from the set I samples. Figure 1 shows the measured critical-current density and

FIG. 1. (a) Critical-current density and (b) flux-pinning force vs perpendicular magnetic field for $d_{Nb} = 290$ Å at three different reduced temperatures.

flux-pinning force for the $d_{Nb} = 290$ Å sample at three different reduced temperatures. J_c is linear near H_{c2}, and is proportional to $H_{c2} - H$. This dependence was used to evaluate H_{c2}^*, the effective upper critical field for the critical-current measurements, and from this to calculate values for $h = H/H_{c2}^*$, the reduced field. (Notice this is a different reduced field from that used in Refs. 4 and 5.) Using this value of H_{c2}^* we can plot the normalized pinning force versus reduced field to see if temperature scaling is obeyed in our samples, as shown in Fig. 2(a). We see excellent temperature scaling except in the region of small h. This loss of scaling is expected since scaling relies on an expansion of the order parameter in powers of h,[7] which fails near H_{c1}. For all samples, the Ginzburg-Landau parameter, κ, is less than 5, and thus H_{c1} is not a small fraction of H_{c2}. We can also see from Fig. 2(b) that not only is temperature scaling obeyed for all the samples of set I, but the shape of the pinning curve is identical between all three.

Usually temperature scaling implies that we can fit the flux-pinning curves to an equation of the form[8]

$$F_p(\mathbf{H},T) \propto g(h)[H_{c2}^*(T)]^n, \quad g(h) = h^l(1-h)^m .$$

From the linear dependence of J_c on $H_{c2}^* - H$ near H_{c2}^*, we might expect that the normalized flux pinning would behave as $h(1-h)$ near $h = 1$, as shown in Fig. 2(a). This seems to hold down to $h = 0.5$. Similar dependencies have been seen for Nb-Ti and Nb-Ta alloys, but the actual shape of $g(h)$ has been found to vary quite
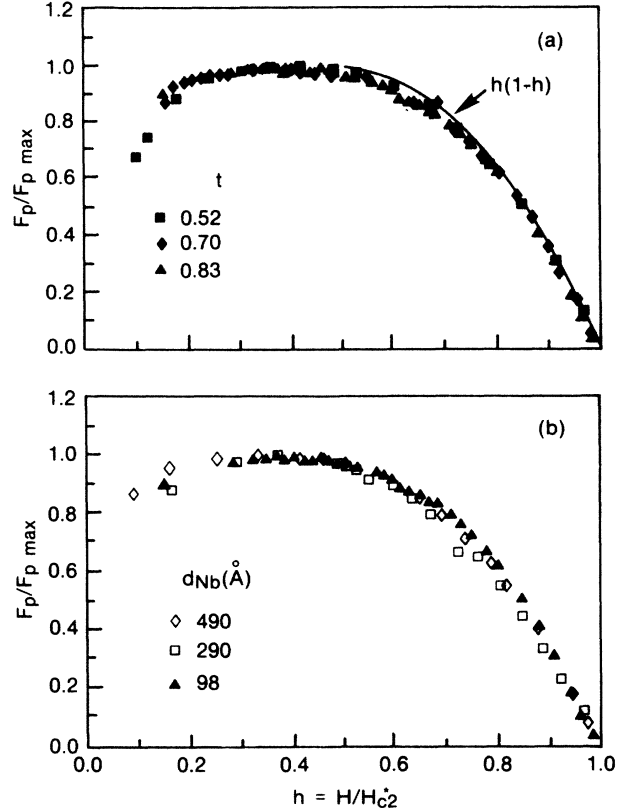

FIG. 2. Normalized flux-pinning force vs perpendicular reduced field curves for (a) $d_{Nb} = 290$ Å at three different reduced temperatures and (b) for $d_{Nb} = 98$, 290, and 490 Å at a reduced temperature of 0.83. The curve is for a $h(1-h)$ dependence normalized to give 1 at $h = 0.5$.

dramatically, depending on the amount of strain in the sample.[8,9]

To obtain the temperature exponent n for these samples, we plot $\log_{10} F_p(T)$ at a constant h versus $\log_{10} H_{c2}^*(T)$, which will give a line of slope n, as in Fig. 3 for $h = 0.45$. We see that for the $d_{Nb} = 290$ and 490 Å samples, $n \approx 2.4$, while for $d_{Nb} = 98$ Å, $n \approx 2.1$. If the pinning mechanism is the same for these samples, as Fig. 2(b) seems to indicate, we might expect the temperature exponent also to be the same. However, it is known that for the same pinning mechanism, n can vary. Talvacchio's work on grain-boundary pinning in Nb_3Sn films[10] found that n depended on the resistivity of the samples, varying from 1.8 for clean samples to 2.5 for dirty samples. If we assume that grain-boundary scattering is the dominant mechanism, then the work on Nb_3Sn would imply that our samples should have resistivities of $> 10 \ \mu\Omega$ cm, based on the measured values of n. From Refs. 4 and 5, however, we know that our samples have low-temperature resistivities of less than 1 $\mu\Omega$ cm. On the other hand, the work of Fietz and Webb on Nb-Ti and Nb-Ta (Ref. 8) showed that pinning by dislocations gives $n \approx 2.5$, and pinning forces of the same magnitude as here.

In addition to the $d_{Nb} = 98$ Å sample having a different value of n, we see from Fig. 3 that while the
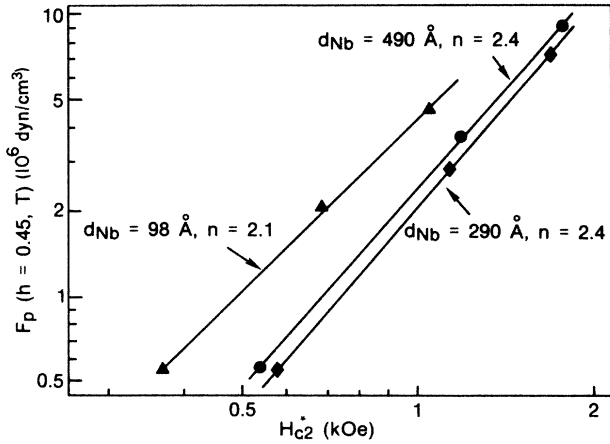
FIG. 3. Log-log plot of $F_p(h = 0.45, T)$ vs $H_{c2}^*(T)$ to determine the temperature-scaling exponent for $d_{Nb} = 98$, 290, and 490 Å.

pinning forces are similar between $d_{Nb} = 290$ and 490 Å, for $d_{Nb} = 98$ Å they are larger by nearly a factor of 2. If the increase in pinning and the decrease in n were due to a mechanism such as a change in the resistivity, then we would expect that the resistivities in the layers would be different for $d_{Nb} = 98$ Å. However, as we have reported earlier,[4] there is little difference among these samples. The overall resistivity for the samples does increase as d_{Nb} decreases, but it varies smoothly, and therefore there should be a smooth variation in the flux pinning among the samples, which is not seen here. This effect is as yet unexplained for our samples.

The size of the pinning forces measured for the samples in set I proved to be larger than expected. Cold-worked Nb-Ta alloys[7] typically have $F_p(h = 0.5, t = 0.7)$ $\approx 1.6 \times 10^6$ dyn/cm^3. For our samples, this value is closer to 3.6×10^6 dyn/cm^3. If our samples are nearly single crystalline, as the work in Ref. 4 implies, why is the flux pinning higher? To study this increase, flux pinning for **H** perpendicular was examined for the samples of set II. Figure 4 shows the maximum flux-pinning force as a function of Λ at $t = 0.83$. We see clearly that the flux pinning increases as Λ increases. For the small-Λ samples, the values of J_c and F_p are very similar to those for cold-worked Nb-Ta alloys. If grain-boundary pinning were present, we would expect the flux pinning to decrease as Λ increases, since the resistivity is decreasing.[5] Therefore, we conclude that grain-boundary pinning is not the dominant mechanism. Another possible explanation for the decrease in F_p as Λ decreases is the fractional increase of Nb-Ta alloy at the interface, which at the measured temperatures may have a lower critical current and pinning force than niobium. Now, although this might explain the data for small Λ, it cannot explain the reduction in F_p for large Λ. Here the fractional change in alloy thickness could only account for a reduction in F_p by a few percent, not the observed reduction by ≈ 1.5.

In addition to the increase in the flux-pinning force, we also see a change in the pinning curve shape as Λ in-
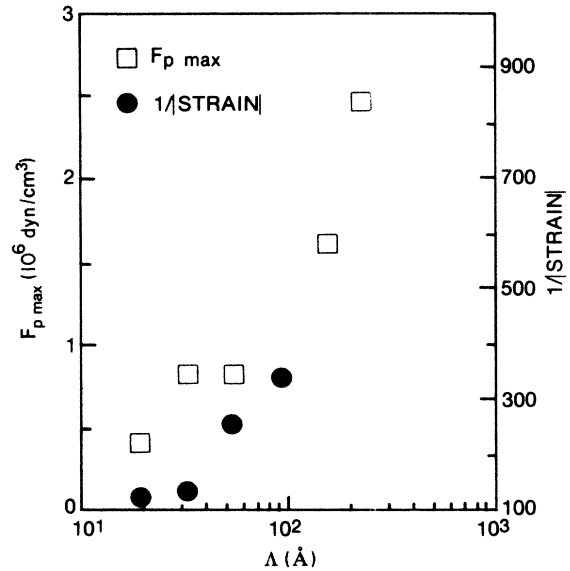

FIG. 4. Maximum flux-pinning force at $t = 0.83$ (squares) and $1/|$ strain $|$ (circles) vs Λ.

creases as shown in Fig. 5. For the large-Λ (> 100 Å) samples, $F_p(h)$ is identical to that seen in the samples of set I, with n being ≈ 2.2. However, for the small-Λ samples, the peak in $F_p(h)$ sharpens and moves to larger h.

A possible explanation of such behavior is the existence of collective pinning[11] for the small-Λ samples which can only manifest itself when the pinning force decreases sufficiently. Collective pinning has been seen in amorphous systems such as Nb-Ge (Ref. 12) and Mo-Ge (Ref. 13). In systems exhibiting collective pinning behavior, there is a peak in the critical current and a sharp peak in the flux pinning near $h = 1$. Figure 6 shows the critical-current density for $\Lambda = 19.5$ Å, verify-
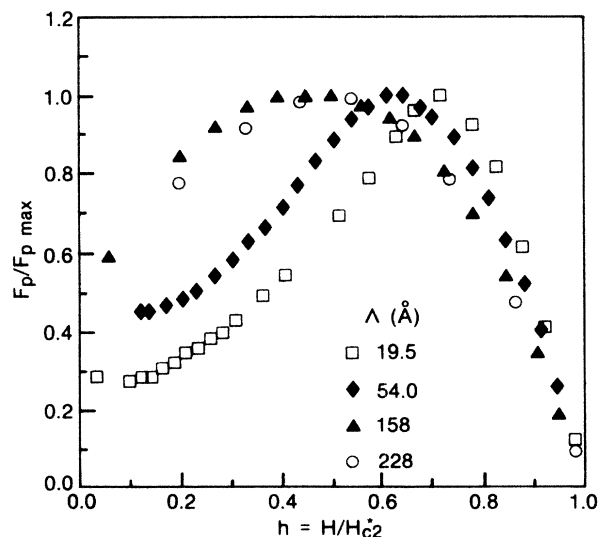

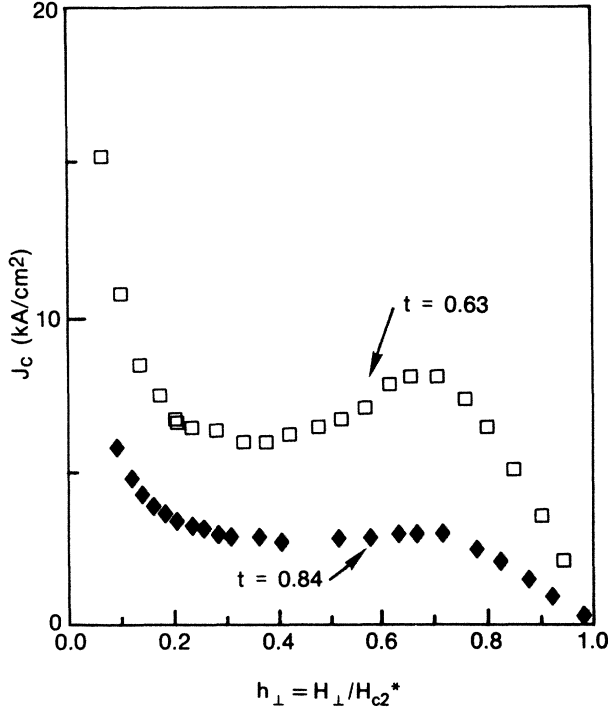FIG. 5. Normalized flux-pinning curves vs perpendicular reduced field for different Λ at $t = 0.83$.

FIG. 6. Critical-current density vs perpendicular reduced field for $\Lambda = 19.5$ Å at two different reduced temperatures. Notice the peak in J_c at $h \approx 0.7$.

ing the existence of a peak near $h = 0.70$. In addition, the maximum flux pinning for $\Lambda = 19.5$ Å at $t = 0.84$ is approximately 0.4×10^6 dyn/cm^3, which is comparable to that seen by Yoshizumi[13] in a-MoGe. So, it is reasonable that this sample exhibits collective pinning.

We will use the equations for two-dimensional (2D) collective pinning[12] to (1) understand the pinning mechanism, and (2) to verify that the sample is in the 2D collective pinning limit. These equations relate the flux-pinning force to a parameter $W(0)$, which in the Larkin-Ovchinnikov (LO) model[11] is expressed by

$$W(0) = n_p \langle f_p^2 \rangle ,$$

where n_p is the density of the pinning centers in the LO model, f_p is the elementary pinning force, and the average is taken over a lattice cell of the flux-line lattice (FLL). In the LO model, the FLL breaks up into correlated regions with a length (L_c) along the field and a length (R_c) perpendicular to the field. In the case of 2D collective pinning, only R_c is important. The condition for 2D collective pinning is given by $L_c \gg d$, where d is the film thickness. From Ref. 12,

$$L_c \approx 3\kappa \frac{\sqrt{h}}{1-h} R_c .$$ (1)

We will use this equation to verify our assumption of the 2D regime.

The flux pinning, correlation length (R_c), and the parameter $W(0)$ are related in the 2D regime by the equations

$$F_p = X^{-1/2}(w/R_c)[W(0)/a_0 d C_{66}] ,$$
$$R_c = X^{-1/2}(w/R_c)[a_0 d^{1/2} C_{66}/W(0)^{1/2}] ,$$ (2)

where w is the film width, d is the film thickness, C_{66} is the FLL elastic constant for shear, $X(y) = 2\pi/(\ln y - 0.029)$ is a logarithmic size correction, and a_0 is the lattice spacing for the FLL, given by

$$a_0 = \left[\frac{2\phi_0}{\sqrt{3}B} \right]^{1/2} ,$$

where ϕ_0 is the flux constant. For the elastic constant, we use the expression developed by Brandt,[14]

$$C_{66}(h, \kappa, T) = \frac{H_c^2(T)}{16\pi} h(1-h)^2(1-0.29h) \exp\left[\frac{h-1}{3\kappa^2 h} \right]$$
$$\times \left[\frac{(2\kappa^2 - 1)2\kappa^2 \beta_0^2}{[(2\kappa^2 - 1)\beta_0 + 1]^2} \right] .$$

Here β_0 is 1.16 for a triangular lattice. We can invert the equations relating $W(0)$ to F_p and R_c to give a set of equations that give the desired quantities, $W(0)$ and R_c, from a measurement of F_p,

$$W(0) = R_c^2 F_p^2 d ,$$
$$R_c = X^{1/4}(w/R_c) \left[\frac{a_0 C_{66}}{F_p} \right]^{1/2} .$$ (3)

To be able to fully use these equations, we must be able to calculate C_{66} from Brandt's expression for our films, which means we must first get an estimate of both κ and $H_c(T)$. This is done using the measured perpendicular critical-field slopes,[5] assuming the Fermi-surface areas are the same throughout the Nb-Ta system, and calculating the strong-coupling enhancement factors from the tunneling results of Hertel et al.[15] Using these results and Eq. (3), we can evaluate both $W(0)$ and R_c for $\Lambda = 19.5$ Å as a function of h, although we must point out that they represent a homogeneous alloy, not a multilayer. In addition, the renormalization of C_{66} due to the disorder in the FLL (as the size of the correlated regions decreases) as described by Kes and Tsuei[12] [which occurs near the peak in $F_p(h)$] will also modify our values. Figure 7 shows the results of this calculation for $\Lambda = 19.5$ Å. In Fig. 7(a), the value of $W(0)$ is plotted versus h along with the predicted dependence from dislocation-loop pinning.[12] Although the fit is not perfect, the agreement must be considered quite good in view of the approximations used. In Fig. 7(b), the calculated values of R_c/a_0 versus h are shown. The values of R_c/a_0 are smaller than in the work of Yoshizumi or Kes and Tsuei. Notice that there is a definite change in the shape of R_c/a_0 at $h \approx 0.75$, which is also where the peak in F_p for this sample occurs, as seen in Fig. 5. Again, this is likely due to the renormalization of C_{66} in the sample. Using these values of R_c in the equation for L_c, we find that the samples are in the 2D limit, with $L_c/d > 10$ for all values of h and t.
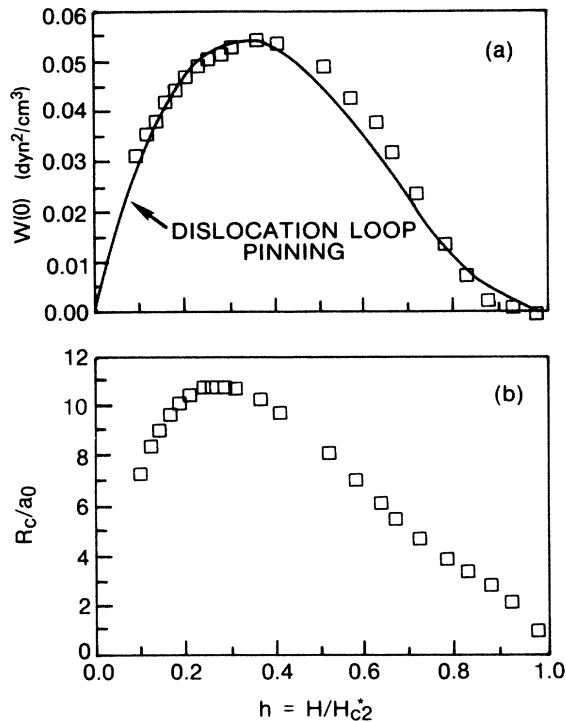
FIG. 7. Values of (a) $W(0)$ and (b) R_c/a_0 vs perpendicular reduced field for $\Lambda = 19.5$ Å at $t = 0.83$. The curve in (a) shows the predicted field dependence for dislocation-loop pinning.

The observations of (1) the field dependence of $W(0)$ for the samples with collective pinning and (2) the increase in the pinning force as Λ increases suggest a model where the pinning is due to dislocations, mediated by the incoherent to coherent driving force in the multilayer lattice. Due to the slight mismatch between the lattice constants of Nb and Ta ($\approx 3 \times 10^{-3}$), there will be a strain both along the interface and normal to it. We can look at this strain for small-Λ samples by looking at the intensities of the satellite peaks around the main Bragg reflection.[16] Figure 4 shows the results of this analysis for $\Lambda = 19.5$, 33.0, 54.4, and 94.1 Å samples [grown on $(11\bar{2}0)$ sapphire], plotting $1/|\varepsilon|$ versus Λ, where ε is the strain along the growth direction. We see clearly that the strain decreases as Λ increases, implying that dislocations are present. This suggests that for the small-Λ samples the misfit at the interface is relieved by strain, while as Λ increases the probability for dislocations increases. Thus, for H perpendicular to the multilayers, dislocation pinning is the dominant mechanism.

H PARALLEL TO THE LAYERS

For this field configuration, the samples in set I were predominantly examined, with some preliminary data taken on the $\Lambda = 19.5$ Å sample. The set I samples were studied since they have the largest values of Λ, and are much more likely to show possible matching effects between the FLL and the multilayer periodicity as described by Ami and Maki.[3] For example, the three

lowest-order matching configurations occur when $\Lambda = \sqrt{3}a_0/2$, a_0, and $\sqrt{3}a_0$, where a_0 is the FLL spacing. Other possible configurations are shown in Ref. 3. As seen in the preceding section, for H perpendicular to the layers, these samples exhibit typical $F_p(h)$ curves showing temperature scaling, etc. For H parallel to the layers, however, the behavior of $F_p(h)$ becomes very complicated.

First, we find that the overall nature of the pinning changes between perpendicular and parallel field orientation. For H perpendicular, $J_c \propto 1 - h$ near $h = 1$, while for H parallel, J_c varies as $(1 - h)^2$. In addition to this and the resulting differences in the shape of F_p, the data for H parallel do not show temperature scaling as seen for H perpendicular. Figure 8 shows the normalized $F_p(h)$ curves for $d_{Nb} = 98$ Å at two different temperatures. We see no evidence of temperature scaling for this sample. As H goes from perpendicular to parallel, there is an increase in both the critical-current density and flux-pinning force. Figure 9 shows the ratio of the critical current and flux pinning between parallel and perpendicular fields for $d_{Nb} = 290$ Å versus temperature at a reduced field of 0.5. Notice that these ratios decrease as the temperature decreases. This decrease in the two ratios and the lack of temperature scaling both fit in with a model of flux pinning due to the layering and dislocations.

The fact that the pinning interaction for parallel fields is different from perpendicular is no surprise. Although pinning by dislocations may still be present, there is also the possibility of pinning due to (1) the surfaces of the films, and (2) the variations in the order parameter from the multilayering along the direction of the driving
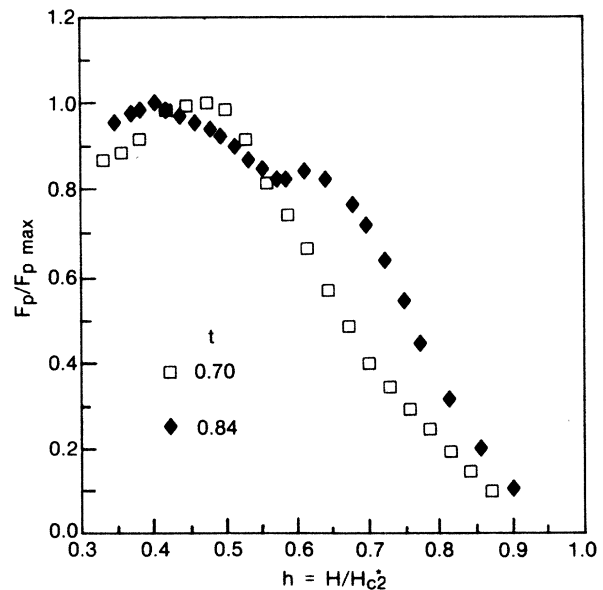

FIG. 8. Normalized flux-pinning curves vs parallel reduced field for $d_{Nb} = 98$ Å at two different reduced temperatures. Notice the lack of temperature scaling.
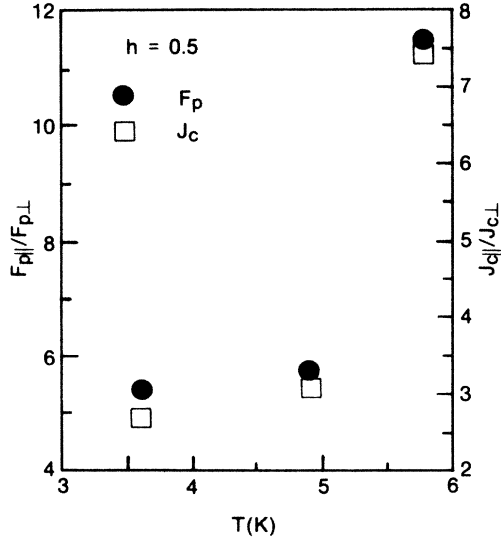
FIG. 9. Ratio of critical current (squares) and flux-pinning force (circles) between parallel and perpendicular field directions at $h = 0.5$ vs temperature for $d_{Nb} = 290$ Å.

force. A vortex in a tantalum layer would find it energetically unfavorable to move into a niobium layer because of the energy cost in keeping the vortex electrons in the normal state. (This is also the same type of mechanism for pinning at the surfaces of the film.) As the temperature decreases, the spatial variation of the order parameter also changes. This change, combined with the different temperature dependence of dislocation-loop pinning, can explain the lack of temperature scaling observed.

The observed temperature dependence of the increase in the flux pinning for parallel fields can also be explained by an additional pinning mechanism on top of that seen for H perpendicular and, in particular, a mechanism due to the multilayering [case (2) above]. The temperature dependence of the pinning due to the variations in the order parameter will depend on the difference in the superconducting condensation energy between the niobium and tantalum layers. As the temperature is decreased towards the T_c of tantalum (4.4 K), this type of pinning will also decrease. This decrease would show up as a reduction in the ratio of the parallel to perpendicular critical currents or flux-pinning force. Such a reduction is seen in Fig. 9. All samples of set I show this behavior, with the ratio of flux pinning between parallel and perpendicular increasing as the temperature is raised above the T_c of tantalum. No correlation between the magnitude of the increase in flux pinning with the number of tantalum layers was observed.

Second, we might see other effects due to the layering, such as matching effects. From Ami and Maki,[3] the matching fields for a triangular lattice will be given by

$$H_m = \frac{\sqrt{3}\phi_0}{2\Lambda^2} \frac{1}{n^2 + m^2 + nm}, \quad n,m = 0,1,2,\ldots \quad (4)$$

For our samples, the first-order matching fields are ≈ 1760, 2950, and 5420 Oe for $d_{Nb} = 490$, 290, and 98 Å,

respectively. Usually these fields are so close to H_{c2}^* that no effect is observed, or in the region of $J_c > 300$ kA/cm^2 and cannot be examined. Therefore, we looked at the higher-order matching fields. The results on the samples are inconclusive. Only $d_{Nb} = 98$ Å ($\Lambda = 575$ Å) shows some evidence of matching, as indicated in Fig. 10 which is a plot of J_c versus H with some of the possible matching fields marked. Interestingly, in the work of Raffy,[2] no peak in J_c was observed until they were below our empirical definition of the 3D→2D crossover point.[5] The $d_{Nb} = 98$ Å sample, however, has structure at temperatures above this value. Higher-order configurations are possible, but they lie close together and are harder to resolve. For conclusive evidence, the first-order matching field should be obtained, either by increasing the spacing ($\Lambda \approx 2000$ Å) or using materials with a higher H_{c2}. We note, however, that if the effect observed here is not due to a matching, then there must be an additional mechanism that causes structure in J_c for H parallel, and not for H perpendicular.

The final feature that might occur for H parallel is the asymmetry in J_c noticed in metal-semiconductor systems by workers at Energy Conversion Devices, Inc. (ECD).[1] This effect is observed as a dependence of J_c on the direction of vortex flow. For H perpendicular, reversing the current direction introduces no change in the measured value of J_c. For H parallel, this is not the case. In the ECD work, they noticed increases in J_c by up to a factor of 2. There is still no clear explanation for this effect. We see similar behavior in our samples as shown in Fig. 11 for $d_{Nb} = 290$ Å at $t = 0.52$. The asymmetry is not as large, being only of order 10%, much smaller than seen in Nb-Si. The asymmetry direction is always the same for different samples, and remains the same under field or current reversal. J_c is always higher for vortex motion away from the substrate. Therefore, if we
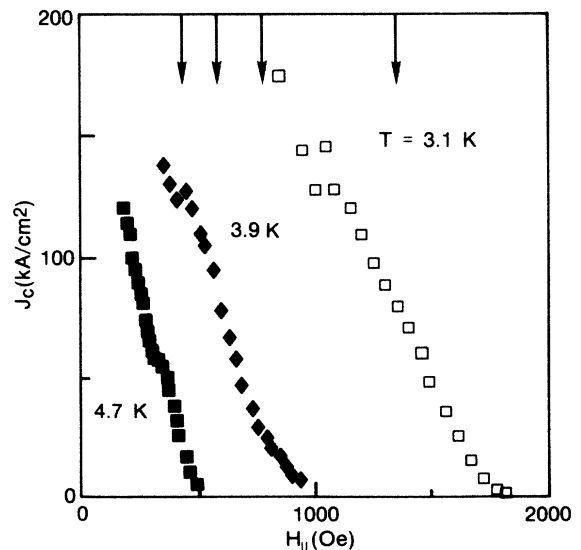

FIG. 10. Critical-current density vs parallel field for $d_{Nb} = 98$ Å at three different temperatures. The arrows mark the location of the matching peaks calculated from Eq. (4).
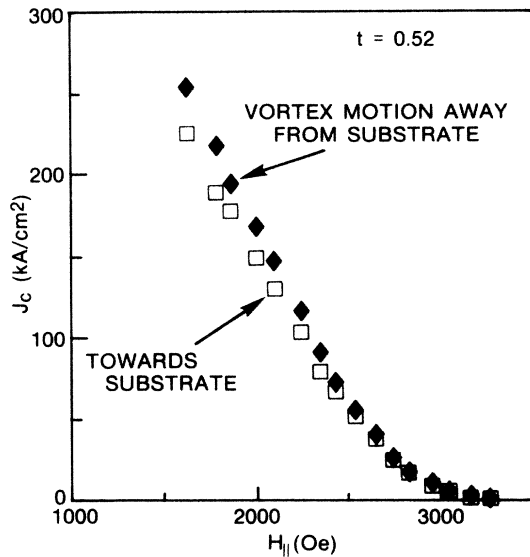
FIG. 11. Critical-current density vs parallel field for $d_{Nb}=290$ Å for opposite orientations of the applied current at $t=0.52$. Notice that J_c is higher for vortex motion away from the substrate.

want to look at this as evidence of pinning from an asymmetric composition profile, then for a vortex in the tantalum layers, the higher pinning is for the Nb on Ta interface. Another explanation is pinning due to the surfaces of the film. Vortices may find it harder to enter from the substrate side than from the vacuum side. It is interesting to note that the ECD work on Nb-Si had the same directional asymmetry, i.e., the hard direction is away from the substrate. This implies that there may be a substantial difference between the upper and lower surfaces of the film. Of course, we see an asymmetry even for temperatures above tantalum's T_c, so the tantalum layers should not present a barrier to flux entry.

This reason for the asymmetry immediately brings up the question of exactly what we are seeing with H parallel to the layers. Are we seeing pinning due to the lay- ered nature, or due to the surfaces of the films? Pinning due to the surfaces could also account for the lack of temperature scaling, but not the decrease in the ratio of the flux pinning between parallel and perpendicular as the temperature decreases. The effects of the layering here are not as dramatic as those seen by Raffy for modulations in the diffusion constant, and the reason for this difference is not understood. More work on critical currents in multilayered systems clearly needs to be done in order to understand better the relationship between the vortex lattice and the multilayer periodicity.

CONCLUSIONS

For H perpendicular to the layers, we have observed pinning in the Nb-Ta multilayered system due to dislocations. The coherent to incoherent driving force results in an increase in the pinning force as Λ increases, which can be related to the observed strain in the samples. For small-Λ samples, the pinning force changes from a single-particle type to a collective mechanism.

For H parallel to the layers, we find an increase in the flux-pinning force and critical current over H perpendicular, which decreases as the temperature decreases. There is a lack of temperature scaling, which is consistent with a model of pinning due to dislocations plus the multilayering. Other effects of multilayering, such as matching and asymmetric critical currents, have proved mostly inconclusive.

ACKNOWLEDGMENTS

*Also at Bell Communications Research, Red Bank, NJ 07701-7020.

[1]A. M. Kadin, R. W. Burkhardt, J. D. Chen, J. E. Keem, and S. R. Ovshinsky, in *Proceedings of the 17th International Conference on Low Temperature Physics, LT-17, Karlsruhe* (North-Holland, Amsterdam, 1984), p. 579.

[2]H. Raffy, J. C. Renard, and E. Guyon, Solid State Commun. **11**, 1679 (1972); **14**, 431 (1977).

[3]S. Ami and K. Maki, Prog. Theor. Phys. **53**, 1 (1975).

[4]P. R. Broussard and T. H. Geballe, Phys. Rev. B **35**, 1664 (1987).

[5]P. R. Broussard and T. H. Geballe, the preceding paper, Phys. Rev. B **37**, 60 (1988).

[6]A. F. Clark and J. W. Ekin, IEEE Trans. Magn. **MAG-13**, 38 (1977).

[7]A. M. Campbell and J. E. Evetts, *Critical Currents in Super-*

conductors (Taylor and Francis, London, 1972).

[8]W. A. Fietz and W. W. Webb, Phys. Rev. **178**, 657 (1969).

[9]G. Fuchs, Phys. Status Solidi A **45**, 239 (1978).

[10]J. Talvacchio, Ph.D. dissertation, Stanford University, 1982.

[11]A. I. Larkin and Yu. N. Ovchinnikov, J. Low Temp. Phys. **34**, 409 (1979).

[12]P. H. Kes and C. C. Tsuei, Phys. Rev. B **28**, 5126 (1983).

[13]S. Yoshizumi, W. L. Carter, and T. H. Geballe, J. Non-Cryst. Solids **61**, 589 (1984).

[14]E. H. Brandt, J. Low Temp. Phys. **26**, 709 (1977).

[15]G. Hertel, D. B. McWhan, and J. M. Rowell in *Superconductivity in d- and f-Band Metals* (Kernforschungzentrum, Karlsruhe, 1982), p. 299.

[16]P. F. Miceli, H. Zabel, and J. E. Cunningham, Phys. Rev. Lett. **54**, 917 (1985).